Hydraulic deterioration due to microbial slime growths

Authors: William G. Characklis, Nick Zelver, and B.F. Picologlou

This is a postprint of an article that originally appeared in Proceedings of the 5th Annual AWWA Water Quality Technology Conference in 1978.

Characklis, W.G., N. Zelver, and B.F. Picologlou, "Hydraulic Deterioration Due to Microbial Slime Growths," in Proceedings of the 5th Annual AWWA Water Quality Technology Conference, Water Quality in the Distribution System, Kansas City, MO, Paper No. 3B-3, 1978.

78-007

HYDRAULIC DETERIORATION DUE TO MICROBIAL SLIME GROWTHS

W. G. Characklis
Assoc. Prof., Environmental Science and Engrg.
Rice University, Houston, Texas 77001

N. Zelver
Research Asst., Environmental Science and Engrg.
Rice University, Houston, Texas 77001

B. F. Picologlou
Asst. Prof., Mechanical Engrg. and Materials Science
Rice University, Houston, Texas 77001

ABSTRACT

Experiments on biofouling development and its effects on frictional resistance are presented. Physical properties of biofilm and kinetic expressions for nutrient uptake as functions of flow conditions are discussed. Also included is a discussion of mechanisms for increased frictional resistance due to biofilms and the dependency of maximum frictional resistance on flow conditions.

INTRODUCTION

Fouling, the undesirable deposition of materials on surfaces, results in significant energy losses in fluid transport systems. Energy loss occurs due to increase in frictional resistance to flow within equipment and piping resulting in decreased capacity for gravity flow systems, or greater power consumption in pumped systems. The general term fouling can reflect any or all combinations of precipitation (scaling), sedimentation, corrosion, and biological (or organic) fouling. This paper concerns biological fouling (biofouling) and, in particular, microbial fouling; its growth in an experimental system and its effect on frictional resistance.

Biological fouling consists of development of thin, microbial films, sometimes followed by a succession of higher life forms. Deterioration of pipeline capacity attributed to biofilm development can be substantial. Seifert and Kruger (1) report a 55% reduction of original capacity in a 61 cm ID, 80 km long water supply line due to a thin slimy layer approximately 650 μm thick; the loss could not be explained by a decrease of effective internal diameter alone. Table 1 documents several other case histories of biofouling in water supply lines.

EXPERIMENTAL METHOD

The objective of this research program was the observation of biofouling film development and the resultant frictional resistance increase within pipelines. Field and laboratory experiments have been conducted to allow a comparison between laboratory-developed films and actual biofouling in terms of formation rate and physical properties.

Invited presentation at the AWWA Water Quality Technology Conference, "Water Quality in the Distribution System," Kansas City, Mo., Dec. 4-7, 1977.

Experimental Apparatus

Laboratory experiments have been conducted using a tubular fouling reactor (TFR) which consists of a fermenter and a 1.27 cm ID glass recycle line (Figure 1). Advantages of this design are as follows:

1) At the high recycle rates employed ($Q' >> Q$), the reactor contents are completely mixed and there are no concentration gradients. This simplifies the mathematical description and sampling, ensures a uniform biofilm in the recycle section and allows for easy control of temperature and pH.

2) A short hydraulic retention time (15 min) can be maintained to eliminate biomass production in the bulk fluid, thus restricting microbial activity to the reactor surfaces.

3) Wall shear stress is independent of the hydraulic retention time.

A detailed drawing of the reactor is shown in Figure 2. Recycle flow rate is maintained at a constant rate during an experiment by an electronic feedback system controlling a positive displacement screw pump. Fouling indicators include biofilm mass, biofilm thickness and change in pressure drop (ΔP) along a fixed length of pipe. Temperature is controlled within $\pm$ 0.3°C, pH is maintained at 7.0 $\pm$ 0.1 and aeration in the fermenter maintains aerobic conditions. Dilution water consists of tap water passed through a carbon adsorption column and substrate feed consists of a 1:1 weight ratio of glucose and trypticase soy broth. Reactor surface area is 9185 cm^2 and reactor volume is 6.6 l.

Field fouling experiments have been conducted on the Houston Ship Channel and an inland lake in Thompson Corners, Texas. The field fouling unit (FFU) consists of four parallel, once-through, glass reactors 1.27 cm ID and 240 cm long (Figure 3). Fouling is indicated by film mass measurement and pressure drop along each reactor. A comparison of laboratory and field water quality data is shown in Table 2.

Fouling Indicators

Film Thickness. Average film thickness measurements in the TFR are conducted on removable sections (5 cm long) which form an integral part of the recycle line. The fouled test section is immersed in a cylindrical vessel filled with a water-surfactant solution. Displacement of the liquid level yields a volume measurement. The difference between the fouled test section volume and the volume of the same section cleaned is the film volume. Wet thickness is determined from film volume and the known surface area of the test section. Precision, based on repeated volume displacement measurements with a clean test section, is $\pm$ 9 μm.

Mass and Density. The fouled test sections described above are dried and weighed. The difference in mass between the fouled test section and the same section after cleaning is the dry film mass. Division by the volume yields a wet mass density and division by the surface of the test section gives areal mass density.

Pressure Drop. Pressure drop measurement is an indirect measure of fouling and is easily converted to a friction factor value. Pressure drop is measured along a 232 cm section of the recycle line with a U-tube mercury manometer and the Fanning friction factor is calculated by the following equation:

$$f = 0.5 \frac{D}{L}\left[\frac{\Delta P}{\rho V_m^2}\right]$$

f = Fanning friction factor

D = tube diameter (L)

ρ = fluid density (M/L^3)

V_m = mean fluid velocity (L/t)

ΔP = pressure drop along length L ($M/L\text{-}t^2$)

Detailed description of all methods can be found elsewhere (2).

RESULTS

Properties of Biofilm

Biofilm properties are "system specific" due to different growth conditions, including limiting substrate and its concentration, temperature and shear stress and varying bacterial populations. In order to minimize the effects of differing starting bacteria populations in the TFR, a standard inoculum was developed. Also, the biofilm thickness and mass measurements are sensitive, to some extent, to the technique employed. Consequently, comparison between results obtained from different investigators is difficult. With these limitations in mind, a composite of physical, biological and chemical properties of biofilm is presented in Table 3.

Chemical properties were obtained from the literature of fouling case histories reviewed by Characklis (3, 4). Inorganic composition of films varies considerably and will most probably affect film properties. Calcium, magnesium and iron have been implicated in film bonding strength (3). Analysis of carbon, nitrogen, and phosphorous of TFR films is shown in Table 4 along with analysis of field biofilm reported by Anderson (5).

Biofilm density (ρ_f) in the TFR (dry film mass per wet film volume) shows a dependency on shear stress at the wall (τ_w); under conditions of constant flow rate, τ_w increases with ΔP as the biofilm grows. The values for τ_w reported here are those for a clean system (initial condition):

$$\rho_f = 6.7 \exp(0.14 \tau_w)$$

Figure 4 indicates the effect of shear stress on film density. The increase in film density with increased shear stress suggests either selective attachment and growth of only certain bacteria from the available population or organism response to the environmental stress.

The dynamic viscoelastic moduli of biofilm grown in the laboratory are reported in Table 5. The results indicate a lightly cross-linked gel. The elastic moduli are of the same order of magnitudes as those of other biological cross-linked protein gels with the same water content (for example fibrinogen networks). The viscous moduli, however, are much larger than the corresponding viscous moduli of similar biological gels.

BIOFOULING DEVELOPMENT

The typical development of biofouling in the TFR and FFU as measured by an increase in film thickness or Fanning friction factor with time is depicted in Figure 5. During the growth phase, a logarithmic increase is evident which may last one to two days in the laboratory and as long as five to fifteen days in the field. At low TFR substrate concentrations (5 mg/l) and in some FFU experiments, the growth phase was not completed and a plateau was not reached during the experimental run time.

The induction period or initial attachment is known to be dependent on surface properties (6). This research is not considering the effects of tube materials or initial attachment phase on the subsequent biofilm growth. To minimize such effects and to ensure uniform induction periods for all experiments, cleaning procedures consisting of a strong base wash followed by a strong acid wash were established. Such procedures were dictated by the fact that the degree to which the glass has been cleaned of organic material has a substantial effect on the adsorption capacity of the glass (7).

Glucose Removal - TFR

Glucose concentrations were monitored by the semimicro method for glucostats. A material balance for glucose in the TFR system is as follows:

$$V\frac{dC_s}{dt} = Q(C_{sog} - C_s) - (M_B)\frac{\mu_{max}}{Y}\left(\frac{C_s}{K_s + C_s}\right)$$

where V = volume of the reactor (L^3)

C_s = reactor glucose concentration (M/L^3)

C_{sog} = input glucose concentration (M/L^3)

Q = substrate feed rate (L^3/t)

M_B = metabolizing biomass (M)

μ_{max} = maximum reaction rate (t^{-1})

Y = yield (biomass produced/substrate uptake)

K_s = saturation constant (M/L^3)

In the above equation, reaction rate has been assumed to follow saturation kinetics:

$$\mu = \mu_{max}\left(\frac{C_s}{K_s + C_s}\right)$$

At steady state, namely when C_s ceases to vary with time, one has

$$Q(C_{sog} - \overline{C}_s) = M_B \frac{\mu_{max}}{Y} \left(\frac{\overline{C}_s}{K_s + \overline{C}_s} \right)$$

where $\overline{C}_s$ = glucose concentration at steady state (M/L^3).

Kornegay and Andrews (8) showed biomass in a completely mixed flow annular reactor to be a function of the reactor area (A), film density (ρ_f) and an "active" film thickness (TH_a).

$$M_B = \rho_f \, A \, TH_a$$

The "active" thickness is considered to be a layer of metabolically active organisms adjacent to the liquid phase. The "active" thickness is defined to be the film thickness at the point where substrate utilization reaches a steady state and is not affected by additional film accumulation.

Preliminary data for the TFR are not sufficient for accurate determinations of an "active" thickness, yield and μ_{max}. Nevertheless, a saturation kinetic expression emerges for all experiments, namely:

$$Q(C_{sog} - \overline{C}_s) = \frac{K(\overline{C}_s - 0.35)}{K_s + (\overline{C}_s - 0.35)}$$

where $K = \frac{\rho_f \, A \, TH_a \, \mu_{max}}{Y}$.

The constant K represents maximum glucose uptake. The constant 0.35 is included because no glucose removal occurred below a glucose concentration of 0.35. Figure 6 shows the experimental points and the saturation curves for different shear stress conditions. It is obvious from this data that K is a function of γ_w. This dependence can come about through the dependence of any or all of ρ_f, μ_{max}, Y, TH_a on γ_w. The variation of ρ_f with γ_w reported earlier in this communication is not sufficient to account for the variation of K with γ_w. This fact leads to the conclusion that one or all of μ_{max}, TH_a and Y are functions of γ_w. Further experiments are necessary to explore this fact.

Atkinson and Davies (9) imply that a diffusional resistance can exist in a microbial film mass. How (10) indicates that Kornegay's model must be modified to account for the effects of the substrate concentration on the "active" thickness. The inclusion of diffusional resistance would require K in the previous equation to be dependent on $\overline{C}_s$. The preliminary data are insufficient to isolate such diffusional considerations.

HYDRAULIC DETERIORATION DUE TO BIOFOULING

Increase in frictional resistance due to biofilms is much greater than that expected from a decrease in pipe radius equal to the film thick-

ness. Figure 7 shows the increase in pressure drop with time and the pressure drop calculated for a clean tube of decreased radius equal to the film thickness. Explanation for the pronounced increase in frictional resistance may be sought in any or all of the following mechanisms:

1) An increase in apparent roughness due to the irregular nature of the film morphology.

2) An interaction between flow and biofilm causing a rippled surface and leading to a further increase in apparent roughness.

3) Resonant vibration leading to energy dissipation within the biofilm due to its viscoelastic nature (11).

Turbulent pipe flow may be divided into three regimes (hydraulically smooth, transitional, and completely rough) depending on the effects of the surface roughness. Determination of the flow regime depends on the relative size of the viscous sublayer (δ_1) and the height of the roughness elements of the wall. The height is characterized by the equivalent sand roughness (k_s). When $k_s < \delta_1$, the pipe appears to be hydraulically smooth. When $k_s > 14\delta_1$ flow regime is fully rough while the transition regime exists when $14\delta_1 > k_s > \delta_1$. The thickness of the viscous sublayer δ_1 is given by

$$\delta_1 = \frac{5D}{Re}\left[\frac{f}{2}\right]^{-0.5}$$

where $Re = \frac{V_m D}{\nu}$ = Reynolds number

ν = kinematic viscosity (L^2/t)

Equivalent sand roughness at initial conditions and at maximum Fanning friction factor attained are shown in Table 6. The equivalent sand roughness is calculated by the following equation (12):

$$k_s = \frac{D}{2}\left[10^{(0.87-0.25/\sqrt{f})} - \frac{9.35}{Re\sqrt{f}}\right]$$

Examination of Table 6 shows that the flow regime for all laboratory runs changes from hydraulically smooth for the clean tubes to transitional or fully rough regimes at the maximum attained Fanning friction factor.

The implication of this discussion is that the biofilm will have no influence on the frictional resistance until surface irregularities protrude through the viscous sublayer. If one assumes that the surface irregularities are of the order of magnitude of the biofilm thickness, this argument leads to existence of a critical biofilm thickness (TH_{crit}). The above assumption is supported by our measurements which show that the thickness of the viscous sublayer for the flow rates studied is between 35 and 70 μm which corresponds well with biofilm thickness at the onset of increasing Fanning friction factor.

It should be stressed that there cannot be a unique relationship between equivalent sand roughness (k_s) and biofilm thickness, as the possibility exists for thick and smooth or thin and irregular films. Consequently, there exists no unique relationship between film thickness and Fanning friction factor. This fact is supported by our measurements as there were instances of decreasing thickness with increasing pressure drop and other instances of decreasing pressure drop with increasing thickness. Possible explanations for these observations are the following:

1) Substantial sloughing of a biofilm may increase surface roughness and produce a greater frictional resistance even though thickness and mass are decreased.

2) A biofilm may become less irregular after growth occurs between the roughness' elements.

Fouling Rate

Fouling rates are calculated from Fanning friction factor data during the logarithmic growth phase (Figure 5). The difference in $\log_{10}$ f values divided by time gives a fouling rate value (R_f). Experiments in the laboratory show fouling rate to be dependent on shear stress at the wall (τ_w) and substrate loading rate (C_{so}). This is shown in Figure 8. The data indicate that the effect of C_{so} on biofouling rates can be described by saturation kinetics of the form:

$$R_f = \frac{R_f^* C_{so}}{R_s + C_{so}}$$

where R_f = fouling rate (t^{-1})

R_f^* = maximum fouling rate (t^{-1})

R_s = saturation constant (M/L^3)

C_{so} = feed substrate concentration (M/L^3)

Preliminary data does not allow determination of the constants R_f^* and R_s.

The field data indicate that a maximum fouling rate may exist with respect to τ_w (Figure 9). A possible explanation for this phenomenon is the competition between diffusion of substrate to the film (increasing fouling rate) and shearing off of the film (decreasing fouling rate). Further experiments in the laboratory are attempting to verify this phenomenon. As expected, the rate of change in Fanning friction factor is much greater in the laboratory due to idealized conditions (Table 7).

Extent of Fouling

The extent of fouling as expressed by maximum Fanning friction factor is primarily a function of τ_w in both the laboratory and the field as indicated in Figure 10. Only TFR results from experiments employing 5-20 mg/l feed substrate are presented since they more closely represent field conditions. The laboratory data was fitted by regression analysis with the following results:

$$f_{max} = 0.00344 \exp (3.53 \tau_w^{-0.5})$$

Since the field fouling data were not used in the regression analysis, Figure 10 indicates that the laboratory system simulates the FFU quite well in regard to maximum Fanning friction factor.

CONCLUSIONS

Analytical techniques and experimental systems have been developed and tested for quantitatively determining biofilm development and its effects. Laboratory results have been compared to field data to verify validity of laboratory experiments. Experimentation is continuing but the following conclusions are useful at this time:

1) Extent of biofouling is primarily controlled by wall shear stress in turbulent flow. The possibility exists of an optimum shear stress to minimize biofouling. Pipe size may be critical in the control of fouling; oversized pipes can enhance fouling processes due to lower shear stress for a given flow.

2) Biofilm density depends on shear stress at the wall (calculated for the clean system); a greater shear stress produces a higher density film.

3) Nutrient uptake obeys saturation kinetics with maximum nutrient uptake being dependent on shear stress.

4) Substrate concentration affects the rate but not necessarily the extent of biofouling.

Data collection continues in order to further corroborate these conclusions. More research is necessary to determine effects of inorganic cations, pH, ionic strength, and suspended solids.

ACKNOWLEDGMENT

The authors gratefully acknowledge the following: the Electric Power Research Institute and the National Science Foundation for partial financial support; James Bryers, William Elvey, John Kirkpatrick, Frank Roe, Eileen Swinford for contributions; and Maurine Lee for typing the manuscript.

REFERENCES

1. SEIFERT, L. & KRUGER, W. Unusually High Friction Factor in a Long, Water Supply Line. VDI, 2 92, 189-191 (1950).

2. CHARACKLIS, W. G. Biofouling Film Development and Destruction: Experimental Systems. Microbiology of Power Plant Thermal Effluents Symposium, University of Iowa, Iowa City, Iowa (Sept. 1977).

3. CHARACKLIS, W. G. Attached Microbial Growths. I. Attchment and Growth. Water Res., 7:1113-1128 (1973a).

4. CHARACKLIS, W. G. Attached Microbial Growths. II. Frictional Resistance Due to Microbial Slimes. Water Res., 7:1249-1259 (1973b).

5. ANDERSON, M. R.; VACCARO, R. F.; & TONER, R. C. A New Concept in

Power Plant Operation to Control Slime Bacteria in Steam-Electric Condenser Cooling Systems. Presented at 2nd Annual Biofouling Workshop, Johns Hopkins University, Baltimore, Md. (1975).

6. HEUKELEKIAN, H. Slime Formation in Polluted Waters. II. Factors Affecting Slime Growth. Sewage Ind. Wastes, 28:78-92 (1956a).

7. ZVYAGINTSEV, D. G. Adsorbtion of Microorganisms by Glass Surfaces. Microbiology (USSR), 28:104-108 (1958).

8. KORNEGAY, B. H. & ANDREWS, J. C. Characteristics and Kinetics of Biological Fixed Film Reactors. Final Report. Federal Water Pollution Control Administration, Research Grant WP-01181 (1967).

9. ATKINSON, B. & DAVIES, I. J. The Overall Rate of Substrate Uptake (Reaction) by Microbial Films. I. A Biological Rate Equation. Trans. Instn. Chem. Engrs., 52:248-259 (1974).

10. HOW, S. Y. The Kinetics of Microbial Films. Ph.D. Thesis, University of Wales (1972).

11. SCHUSTER, H. Fluid Friction in the Presence of Non-Rigid Boundaries. Ph.D. Thesis, Johns Hopkins University, Baltimore, Md. (1971).

12. SCHLICHTING, H. Boundary Layer Theory. McGraw-Hill Book Co., New York (1968).

13. MINKUS, A. J. Determination of the Hydraulic Capacity of Pipelines. Jour. New Engl. Wat. Wks. Assn., 68:1-10 (1954).

14. POLLARD, A. L. & HOUSE, H. E. An Unusual Deposit in a Hydraulic Tunnel. Jour. Pwr. A. Soc. Civ. Engrs., 85:PO6:163-171 (1959).

15. ARNOLD, G. E. Crenothrix Chokes Conduits. Engrg. News Rec., 116: 774-775 (1963).

16. WIEDERHOLD, W. Effect of Wall Deposits on Hydraulic Loss in Pipelines. Gas Wass Fach., 90:634-641 (1949).

17. DERBY, R. L. Control of Slime Growth in Transmission Lines. Jour. Am. Wat. Wks. Assn., 39:1107-1114 (1947).

NOMENCLATURE

A	area
C_s	reactor glucose concentration
C_{so}	feed substrate concentration
C_{sog}	input glucose concentration
$\bar{C}_s$	glucose concentration at steady state
D	diameter
f	Fanning friction factor
k_s	equivalent sand roughness
K	maximum glucose uptake
K_s	saturation constant

M_B	metabolizing biomass
Q	substrate feed rate
Q'	recycle flow rate
R_f	fouling rate
R_f^*	maximum fouling rate
R_s	saturation constant
TH_a	"active" film thickness
TH_{crit}	critical biofilm thickness
V	volume of reactor
V_m	mean fluid velocity
Y	yield (biomass produced/biomass uptake)
δ_l	viscous sublayer
ΔP	pressure drop
ρ	fluid density
ρ_f	film density
μ_{max}	maximum reaction rate
ν	kinematic viscosity
γ_w	shear stress at the wall for clean system

TABLE 1

Data Summary from Case Histories of Closed Conduits Experiencing Frictional Losses Due to Slimes

Reference	Minkus (13)	Minkus (13)	Pollard (14)	Arnold (15)	Wiederhold (16)	Derby (17)
Diameter (in.)	42	36	132	36	24	14
Length (miles)	7	7	4.5	22	50	1.25
Surface	Cement	Concrete	Concrete-Steel	Steel	Steel	Steel
Slime thickness (in.)	$\frac{1}{32}$	$\frac{1}{16}$	$\frac{1}{2}$	$\frac{1}{8}$ $\frac{1}{4}$	$\frac{1}{40}$	
Frictional head (ft)			15 ft-(at 900ft^3s^{-1})			
Loss in capacity (as % of design capacity)	12(2 yr)	23		16(3 wk)	55(3 yr)	3.5(1 yr)
Chemical added	*Chlorine		Lime	Chlorine-ammonia		Chlorine
Chemical concentration(mg l^{-1})	50		20	0.7-0.2		9-12

*Accompanied by flushing at 6 ft s^{-1}

TABLE 2

Water Quality Data for Biofilm Experiments

	Bulk Temp (°C)	Bact. (#/ml)	pH	TOC (mg/l)	BOD (mg/l)	SS (mg/l)
Houston Ship Channel	16	10^3	6.4	33	19	100
Lake at Thompson Corners	--	10^3	9.0	21	4	--
Laboratory						
Tap Water	--	--	7.0	8.6	--	--
C_{so} = 5 mg/l	30-40	7.0	7.0	--	2.5*	1.2
12.5 mg/l	30-40	7.0	7.0	--	6.2*	3.0
20 mg/l	30-40	7.0	7.0	18.0	10*	4.8
100 mg/l	30-40	7.0	7.0	54.8	50*	24.1

*estimated value

TABLE 3

Some Properties of Biofilms

PHYSICAL	Flow Conditions During Growth	
	Laminar	Turbulent
Maximum thickness (μm)[a]	1300	1000
Mass density (mg/cm³)	30-100	5-40
Areal density (mg/cm²)	0.5-13.0	0.05-1.5
Solids content (%)	0.5-5.0	0.5-5.0
Rheological character	viscoelastic	viscoelastic
Sloughing characteristics	intermittent	continuous
BIOLOGICAL		
Bacterial cell density (cells/cm³)		10^9-10^{10} (turbulent)
Frequently observed organisms	*Sphaerotilus*	
	Crenothrix	
	Gallionella	
	Pseudomonas	
	Flavobacteria	
	Achromobacter	
	Aerobacter	

CHEMICAL	
Water (%)	85.6 - 95.4
Volatile solids (%)	1.9 - 3.2
Fixed Solids (%)	1.4 - 11.7
Si as % of fixed solids	85.6 - 95.4
Fe " " "	1.9 - 3.2
Al " " "	3.9 - 7.5
Ca " " "	1.0 - 5.6
Mg " " "	2.5 - 3.2
Mn " " "	4.9 - 59.5

[a]Between 20-30° C

TABLE 4

Chemical Analysis of Biofilms Developed in the Laboratory and Field: Carbon, Nitrogen, Phosphorous (% of dry weight)

	Laboratory	Field[5]
Organic carbon	19.0 %	6.4 - 13.8 %
Kjeldahl nitrogen	9.2	0.5 - 3.0
Total Phosphorous	1.8	

TABLE 5

Dynamic Viscoelastic Moduli of Biofilm Grown in the Laboratory Reactor

Excitation Frequency (Hz)	Elastic (Storage) Modulus, G' (N/M^2)	Viscous (Loss) Modulus, G'' (N/M^2)
3.00	54.5	76.2
4.32	51.7	88.7
5.27	53.6	98.4
6.00	59.5	118
7.93	76.4	142
9.80	117	182
12.00	299	368

Temperature was maintained at 40° C and initial shear stress (τ_w) was 5 N/M^2. Substrate Input (C_{so}) consisted of 10 mg/1 Trypticase Soy Broth. The viscoelastic measurements were conducted on a Weissenberg Rheogoniometer.

TABLE 6

Equivalent Sand Roughness Calculations and Corresponding Flow Regimes for Laboratory Experiments

Reynolds Number	Temp. (°C)	Substrate Input (mg/l)	Initial Conditions (clean tube) k_s (cm)	Initial Conditions (clean tube) k_s/δ_1	At Maximum k_s (cm)	At Maximum k_s/δ_1
30800	30	20	0.001	0.272	0.013	4.36
30800	30	100	0.001	0.272	0.208	131
29000	40	5	0.002	0.537	0.023	8.14
29000	40	20	0.002	0.537	0.035	13.4
29000	40	100	0.002	0.537	0.023	8.14
21100	35	12.5	0.00	0.393	0.046	9.45
14600	30	5	0.004	0.589	0.150	35.4
14600	30	20	0.004	0.589	0.078	17.9

TABLE 7

Rate of Increase in log_{10} Fanning Friction Factor

	Δ $\log_{10}$ Fanning Friction Factor x $days^{-1}$
Houston Ship Channel	0.030 - 0.060
Lake at Thompson Corners	0.004 - 0.015
Laboratory	
C_{so} = 5 *mg/l*	0.060 - 0.977
12.5 *mg/l*	0.065 - 0.048
20.0 *mg/l*	0.151 - 0.988
100 *mg/l*	0.214 - 1.351

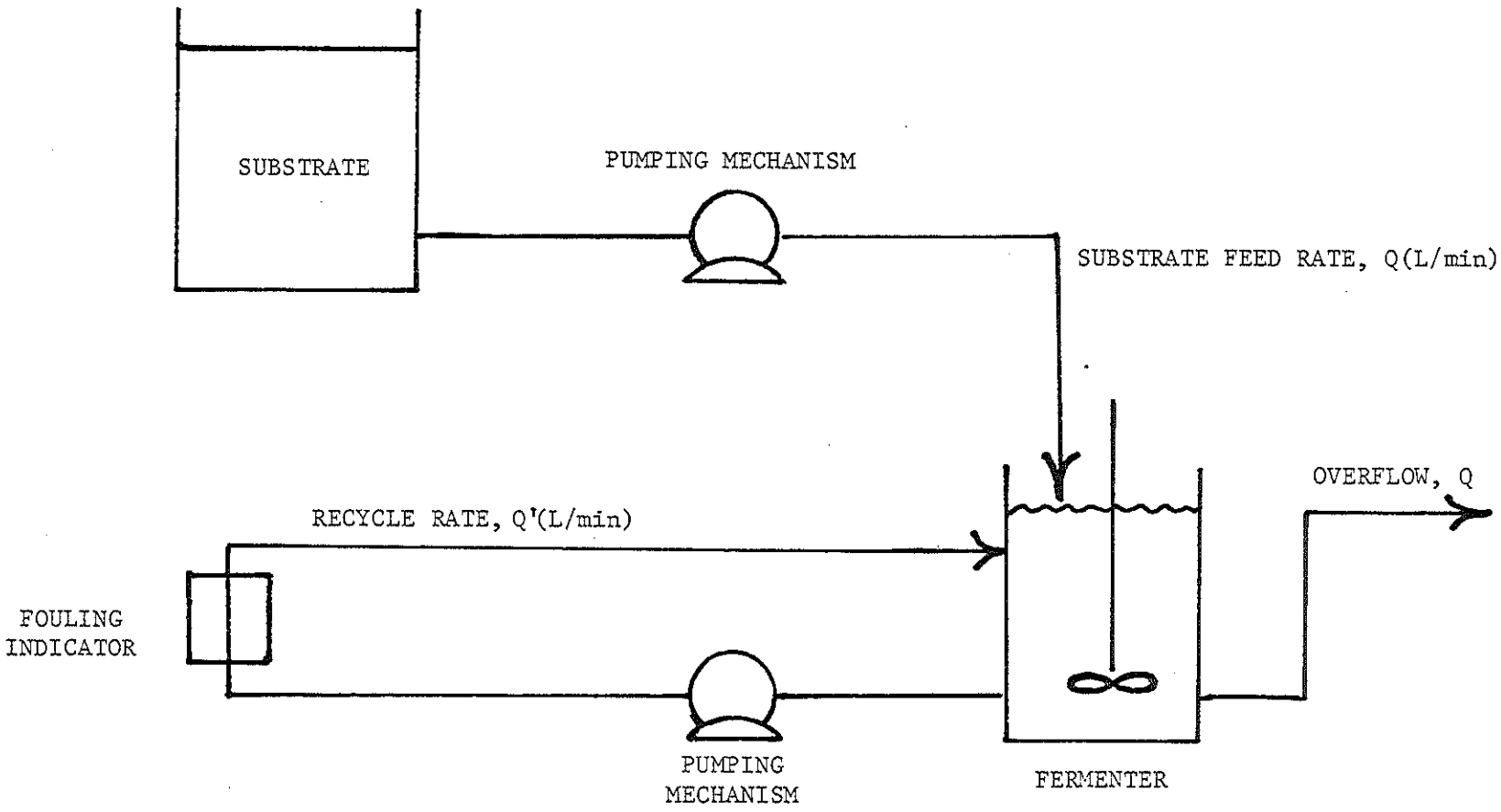

Figure 1. *Schematic Diagram of Tubular Fouling Reactor Apparatus. Note: Q'>>Q and V/Q is less than the suspended Biomass Generation Time.*

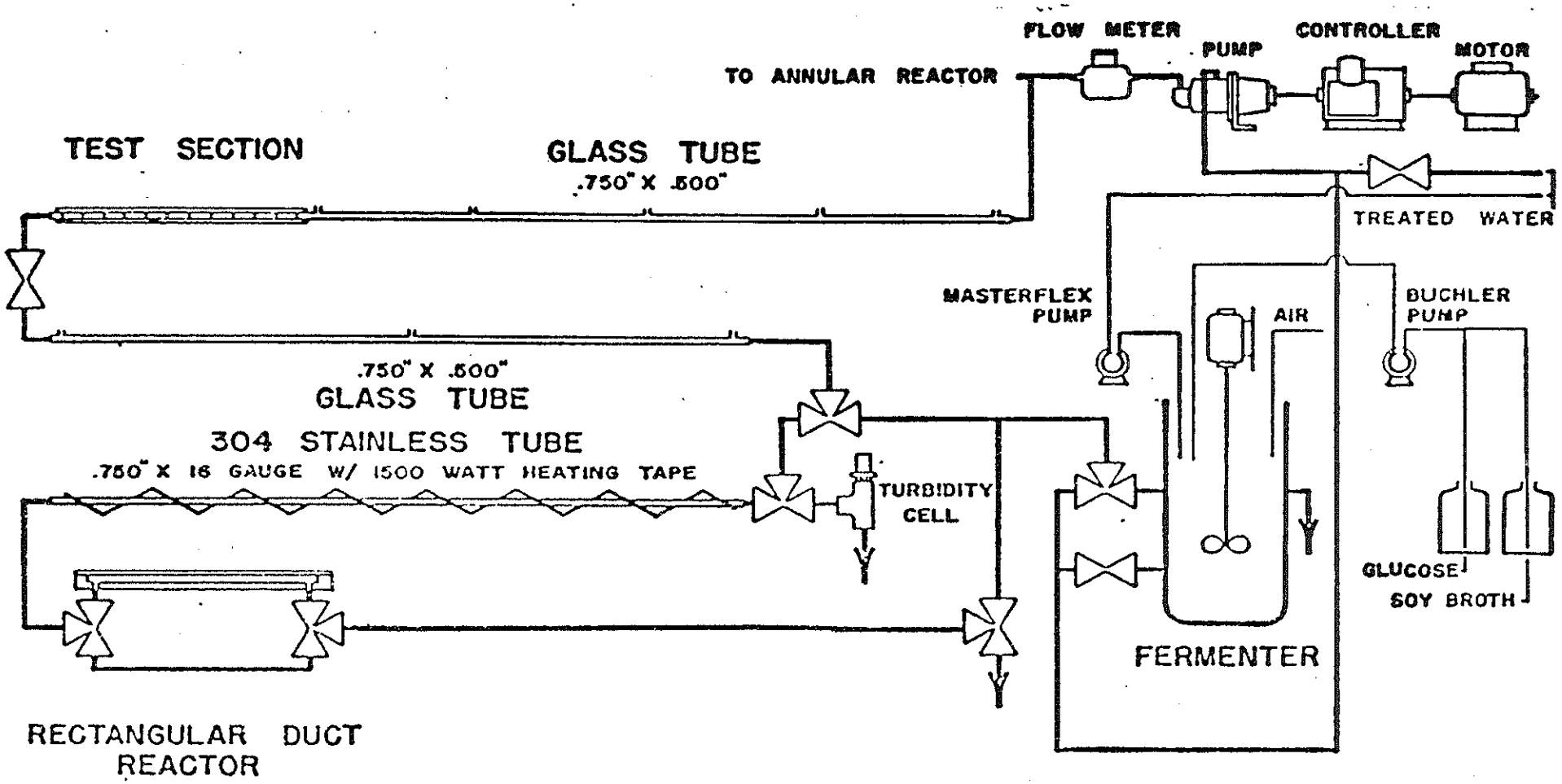

Figure 2. *Tubular Fouling Reactor System*

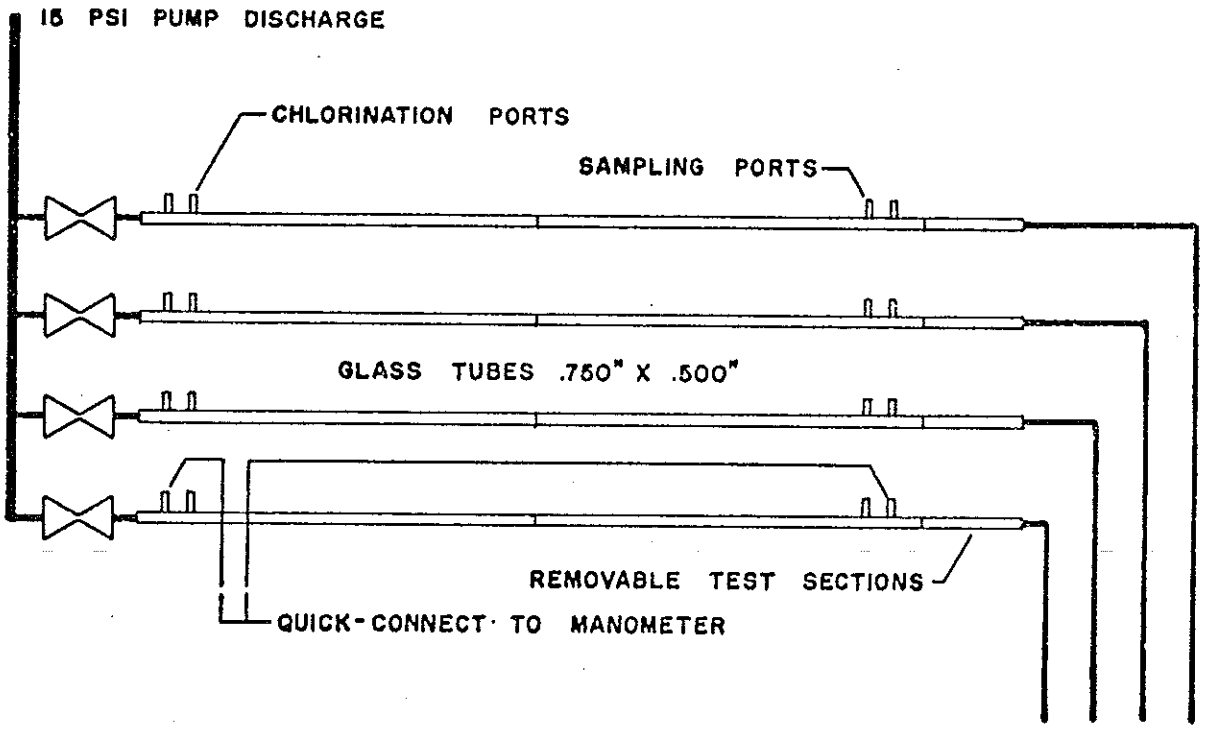

Figure 3. *Field Fouling Apparatus*

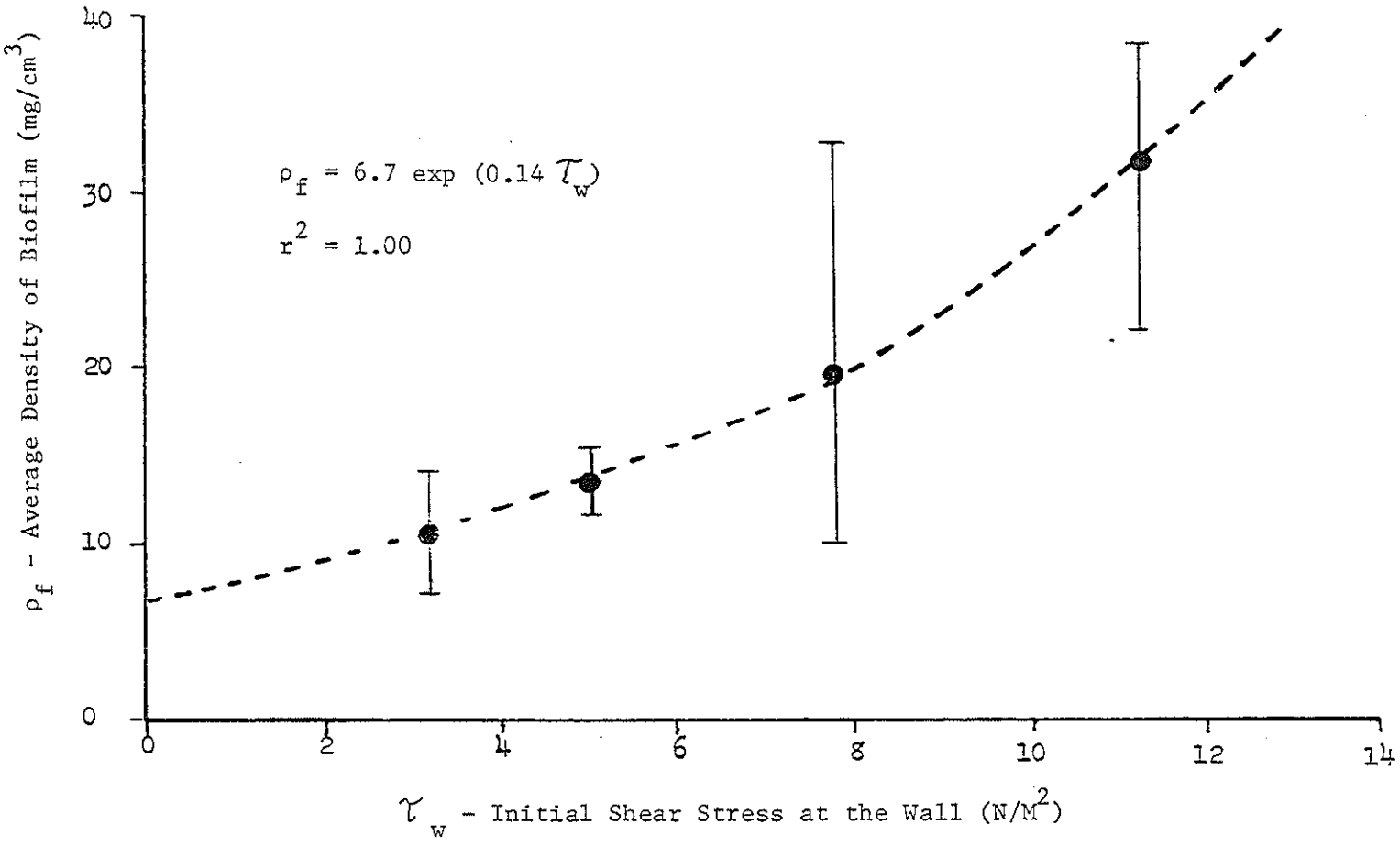

Figure 4. *Change in Film Mass Density with Initial Shear Stress*

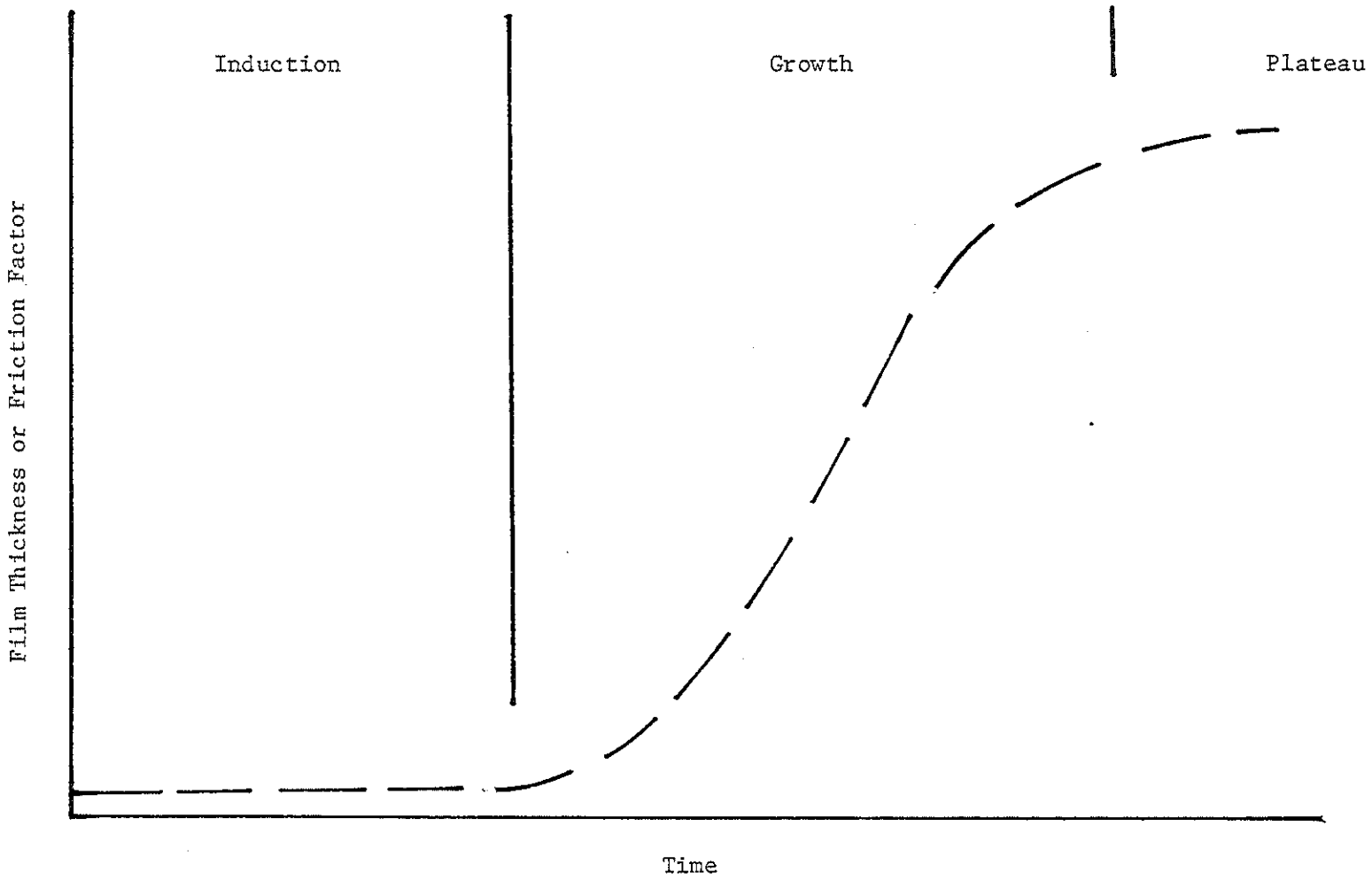

Figure 4 *Progression of a Typical Biofouling Experiment*

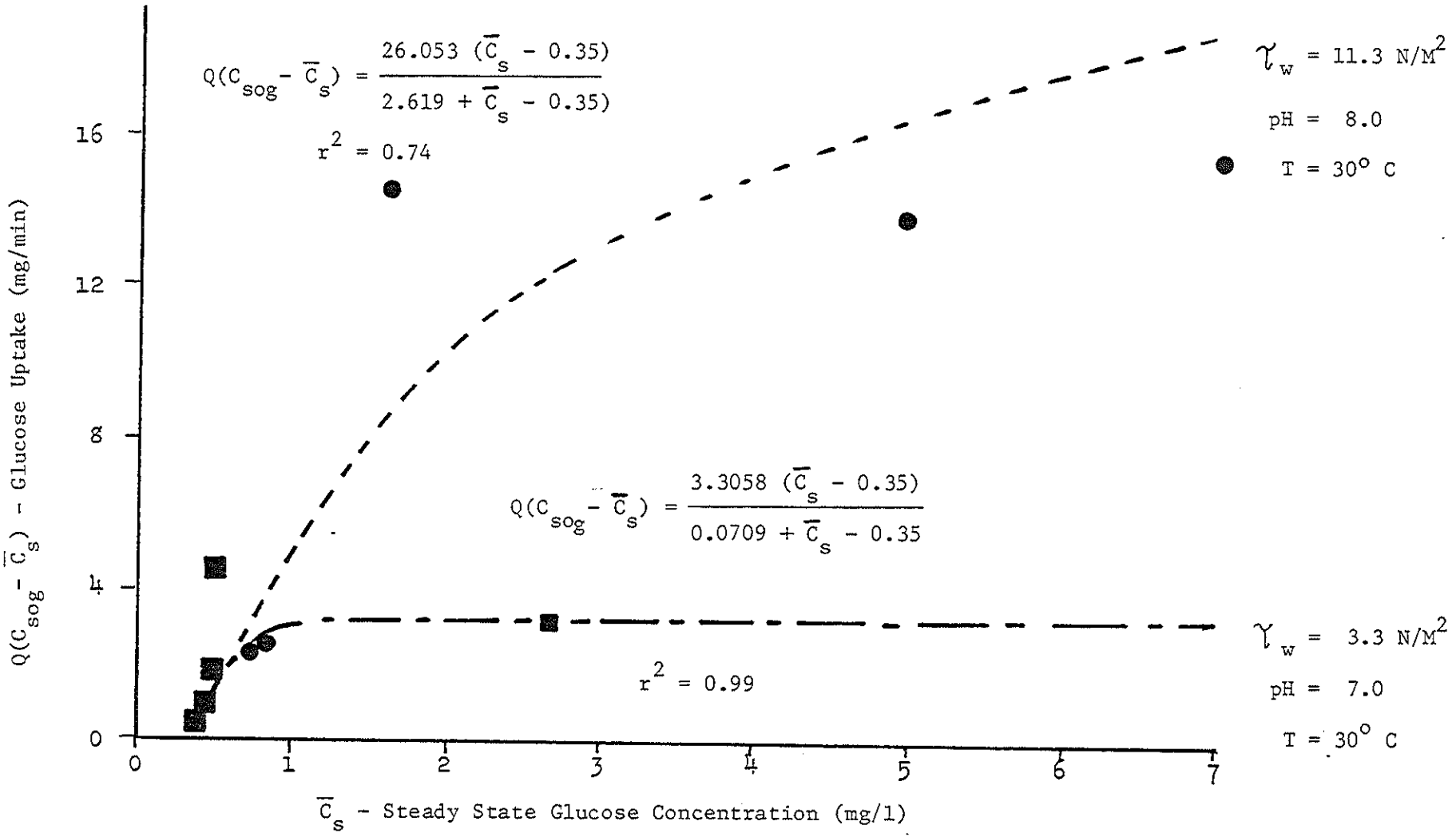

Figure 6. *Glucose Removal Rate at Varied Initial Shear Stress*

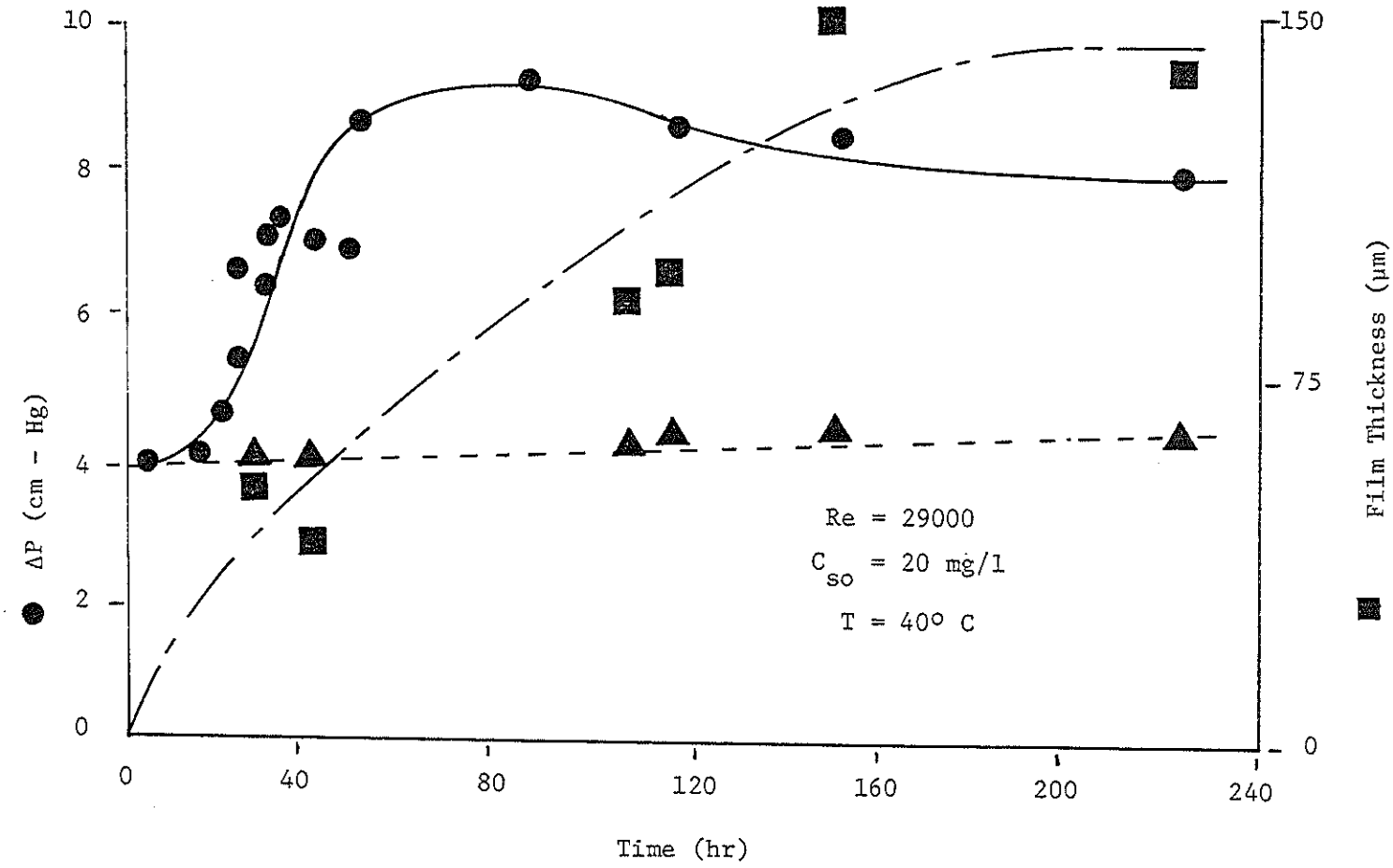

Figure 7. *Increase in ΔP for a TFR Experiment (●) and Corresponding Film Thickness (■). Note the line representing increase in ΔP for a clean tube with a decreased radius equal to the film thickness (▲); this line was calculated using the Blasius Equation*

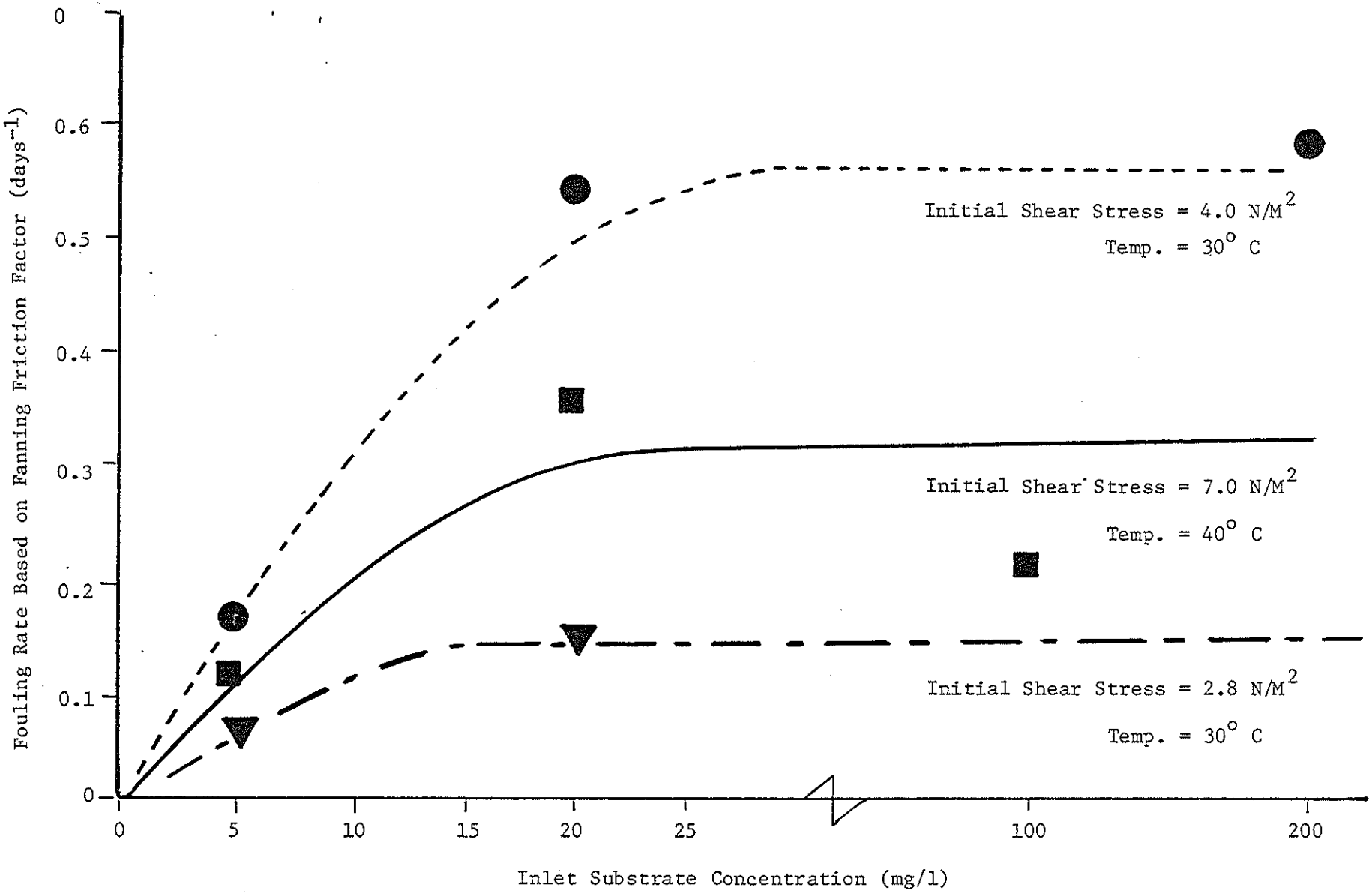

Figure 8. *Fouling Rates vs. Inlet Substrate for Laboratory System*

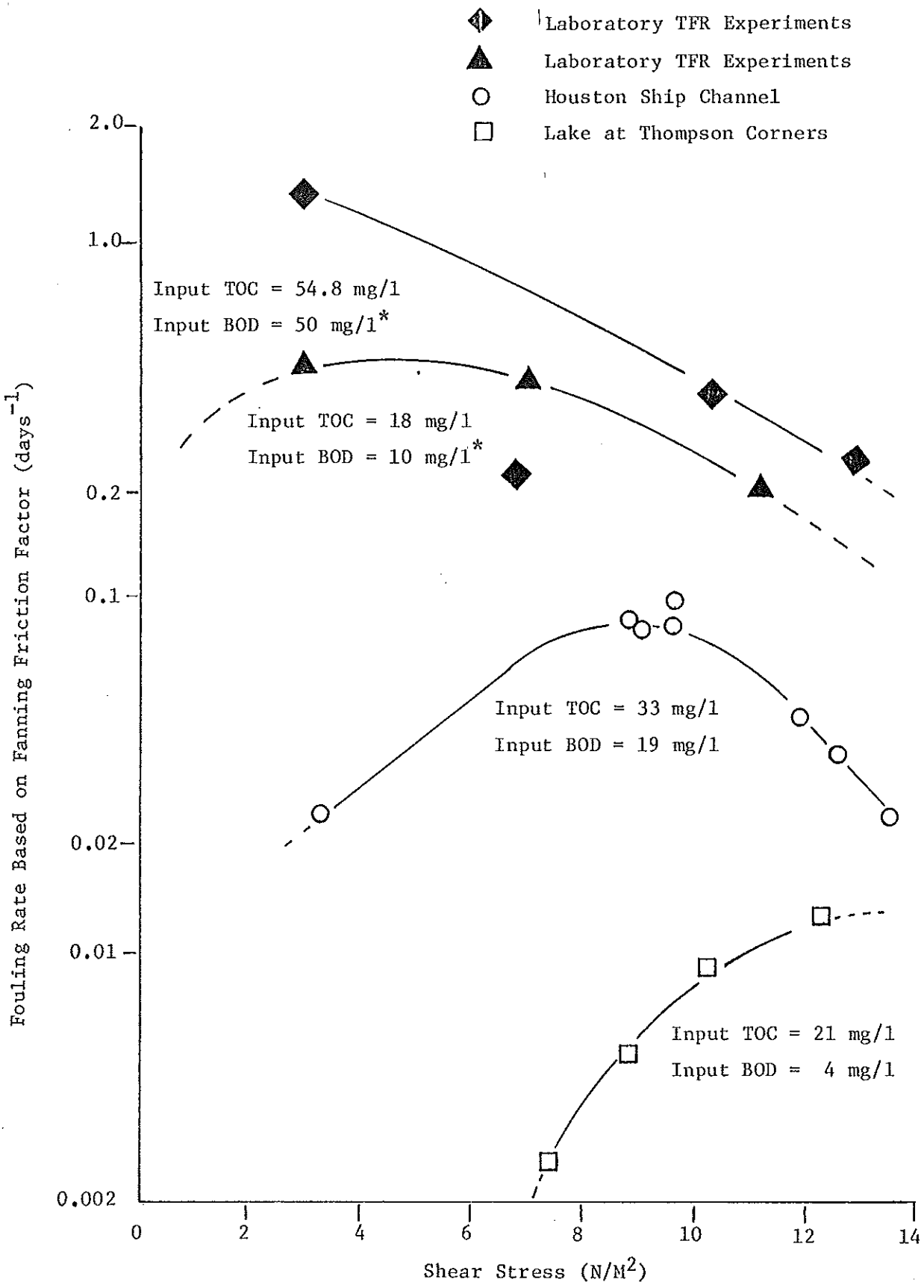

*estimated values

Figure 9. *Fanning Friction Fouling Rates vs. Shear Stress for the Field Fouling Apparatus*

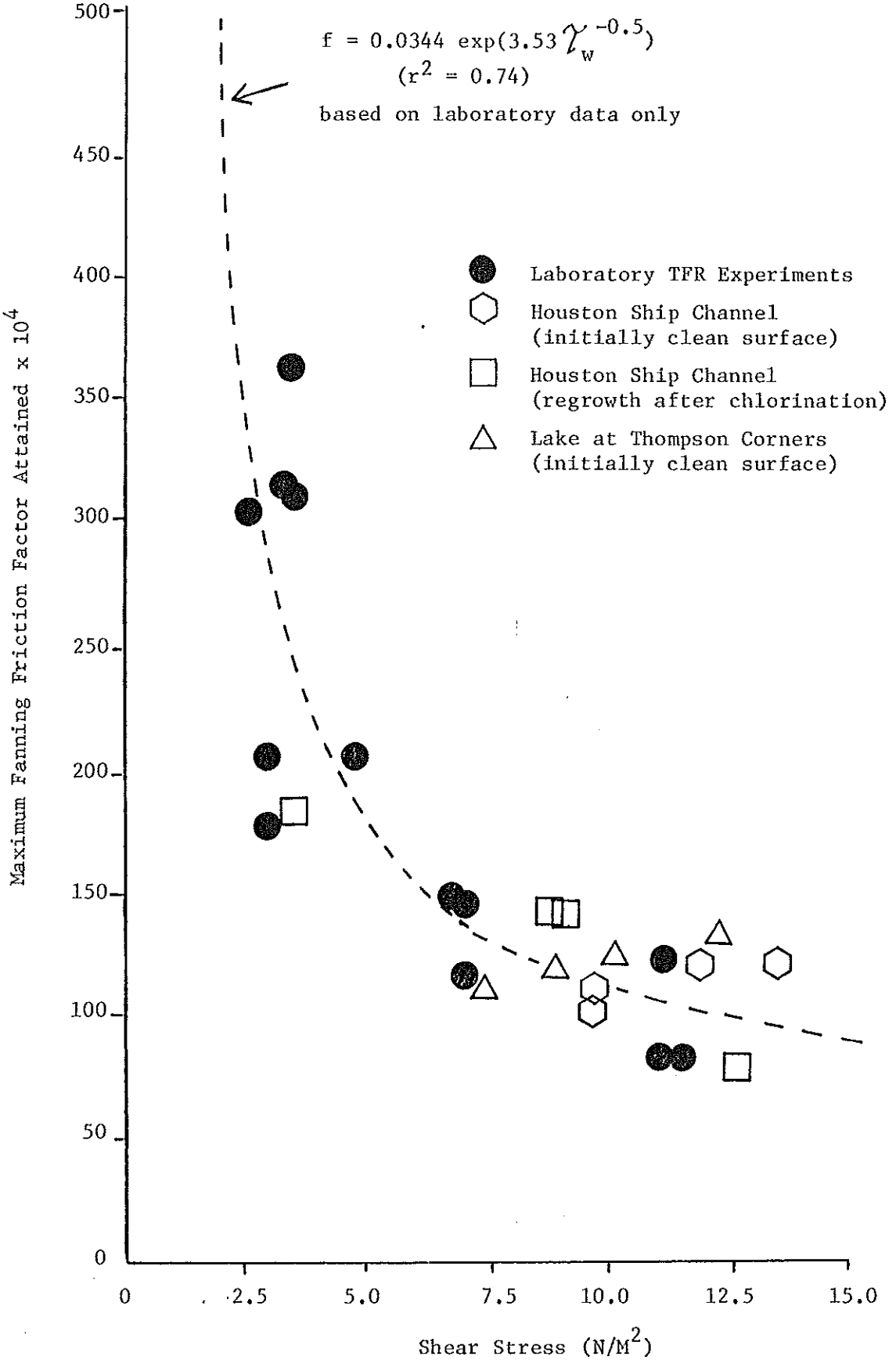

Figure 10. *Comparison of Extent of Fouling in the Laboratory and Field Experimental Systems*